Computational Study of the Lowest Triplet State of Ruthenium Polypyridyl Complexes Used in Artificial Photosynthesis

O. Anders Borg,[†] Sofia S. M. C. Godinho,*[,†] Maria J. Lundqvist,[†] Sten Lunell,[†] and Petter Persson[‡]

Department of Quantum Chemistry, Uppsala University, Box 518, SE-751 20 Uppsala, Sweden, and Chemical Physics, P.O. Box 124, SE-22100, Lund, Sweden

Received: January 4, 2008; Revised Manuscript Received: March 10, 2008

The potential energy surfaces of the first excited triplet state of some ruthenium polypyridyl complexes were investigated by means of density functional theory. Focus was placed on the interaction between the geometrical changes accompanying the photoactivity of these complexes when used as antenna complexes in artificial photosynthesis and dye-sensitized solar cells and the accompanying changes in electronic structure. The loss process ^{3}MLCT → ^{3}MC can be understood by means of ligand-field splitting, traced down to the coordination of the central ruthenium atom.

Introduction

Ruthenium(II)polypyridyl complexes have visible and near-visible light absorption properties that have led to a wide range of applications in photochemistry and photocatalysis.[1,2] In addition to strong absorption, long-enough excited-state lifetimes to initiate electron transfer to neighboring molecules enhances the applicability of several of these complexes as light harvesting antennas in photoactive systems.[1] Two of the most important applications are dye-sensitized solar cells,[3–5] and donor−photosensitizer−acceptor triads in artificial photosynthesis.[2,6–13] The most intense peaks in a Ru(II)polypyridyl UV−vis spectrum correspond to the singlet ground state (S_0) to singlet metal-to-ligand charge transfer (^{1}MLCT) transitions,[1,7,14] commonly abbreviated as ^{1}MLCT ← S_0. The MLCT states are also, typically, the lowest lying excited states since the highest occupied orbitals are of mainly ruthenium 4d character, and the lowest unoccupied states are pyridine π^* orbitals.[15] Ruthenium belongs to the second transition metal series and therefore readily mediates intersystem crossing from ^{1}MLCT to ^{3}MLCT, thoroughly described for $[Ru(bpy)_3]^{2+}$ (bpy = 2,2′-bipyridine) in ref 16.

The stability of the ^{3}MLCT state is crucial for the capability of these complexes to induce further reactions since the excitation energy is carried by the electron transferred to the pyridine π^* orbital.[1,15] The ^{3}MLCT state is depopulated through both radiative and nonradiative pathways,[15,17] but the major deactivation channel at room temperature proceeds over an adiabatic transition state from the ^{3}MLCT state to a metal centered, ^{3}MC, state. This means that the electron initially relocated from Ru to the ligand π^* molecular orbital (MO) is transferred back to the ruthenium center but to a different d orbital than in the S_0 state.[15] Once formed, however, the ^{3}MC state relaxes to the S_0 state. This deactivation, taking place internally in the complex, therefore implies a loss of excited-state energy, and large research efforts have been made toward avoiding this process.

A perfect octahedral environment is well-known to split the frontier d orbitals in a transition metal into two energy levels, the lower (t_{2g}) consisting of d_{xy}, d_{yz}, and d_{xz} and the upper (e_g) consisting of of $d_{x^2-y^2}$ and d_{z^2}. In a sufficiently strong octahedral field, Ru^{2+} has the ground-state electronic configuration [Kr]$4d^6$, with the t_{2g} orbitals occupied and the e_g orbitals unoccupied. A ^{3}MC excited state will therefore have one singly occupied orbital of d_{xy}, d_{yz}, or d_{xz} character and one of $d_{x^2-y^2}$ or d_{z^2} character.

Ligand coordination has been used as a parameter that is believed to affect the excited-state lifetime. The $[Ru(bpy)_3]^{2+}$ complex has been shown to fulfill the requirement of good ligand coordination and also exhibits a long excited-state lifetime, $\tau = \sim 1\ \mu s$.[15,17] This complex has been used as a model system,[19] as well as its most well-known derivate, the so-called N3 dye, Ru(4,4′-dicarboxy-2,2′-bipyridine)$_2$(NCS)$_2$. In the latter complex, one bpy ligand was substituted by two NCS^- ligands to optimize absorption and redox properties, and the two remaining bpy ligands were functionalized by carboxyl groups that are used to anchor the dye to semiconductor surfaces.[5] Albeit being effective as a photosensitizer in both donor−photosensitizer−acceptor triad systems and dye-sensitized solar cells, a monosubstitution of the bpy ligands leads to different ruthenium complex isomers.[20] In, for example, the donor−photosensitizer−acceptor triad, some of these isomers will allow interactions between donor and acceptor due to spatial proximity. Photosensitizers that form linear structures are highly desirable since substituent interactions are prevented. The formation of linear arrangements cannot be easily controlled when using $[Ru(bpy)_3]^{2+}$ as the photosensitizer. In a recently published paper, Abrahamsson and co-workers therefore started from a ligand that allowed a linear arrangement,[18] the tridentate 2,2′:6′,2″-terpyridine (tpy) ligand (Figure 1), as a reference compound when designing a new antenna complex with a longer excited-state lifetime.

Substitution in the 4′-position (lowermost carbon in Figure 1) of the tpy ligand minimizes the possibility for unwanted interactions. The tpy ligand itself has the disadvantage that the lifetime of the ^{3}MLCT state is only 0.25 ns at room temperature.[21] The probability for further reactions or electron transfers is therefore low, and several other tpy-related ligands with extended lifetimes have been suggested.[17,18] By synthesizing

* Corresponding author. E-mail: sofia.godinho@kvac.uu.se; fax: +46 18 471 58 30.
† Department of Quantum Chemistry, Uppsala University.
‡ Chemical Physics.

10.1021/jp8000702 CCC: $40.75
Published on Web 04/22/2008

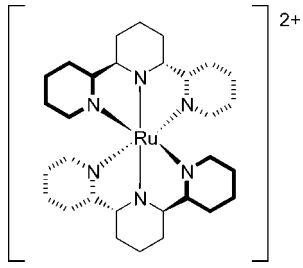

Figure 1. Schematic image of the $[Ru(tpy)_2]^{2+}$ complex.

and testing different types of ligands, finally a lifetime of 3 μs for $[Ru(bqp)_2]^{2+}$, a $[Ru(tpy)_2]^{2+}$ related complex, was obtained (bqp = 2,6-bis(8′-quinolinyl)pyridine).[18]

In this work, we took the first steps in an investigation of the first triplet state potential energy surface (PES) using high-level quantum chemical methods and adequate basis sets. We wanted to further explore the connection between ligand coordination, photostability, and thermodynamics of the first triplet state of these complexes. We began by studying $[Ru(tpy)_2]^{2+}$ as the reference complex. The *cis*-$[Ru(bpy)_2(py)_2]^{2+}$ complex, with a lifetime of the lowest triplet state equal to 500 ns, increasing the lifetime by a factor of 2000 when compared to our reference complex, is a good model to test the influence of coordination of the central metal ion, with a minimum of alteration of the ligand. Further improvement on ligand octahedral coordination by the introduction of two other tridentate ligands was observed in the last studied complex, $[Ru(pmp)_2]^{2+}$, and the one showing a lifetime of the lowest triplet state equal to 3 μs, $[Ru(bqp)_2]^{2+}$.

We assumed that the coordination of the metal center in the ^{3}MLCT state is more important than that in S_0, and conclusions should be drawn from that structure and not from S_0. The structure of S_0 is much more readily experimentally determined than the structure of T_1. By means of quantum-chemical calculations, we here assessed the structure in the T_1 state and compared the coordination to that in the ground state. In addition, the geometrical alterations accompanying the $S_0 \rightarrow {}^3$MLCT $\rightarrow {}^3$MC process were investigated for $[Ru(tpy)_2]^{2+}$, and a detailed electronic structure explanation is provided for the geometrical changes.

With an elaborate investigation of the electronic structure of $[Ru(tpy)_2]^{2+}$ as a reference, the excited-state chemistry of the related *cis*-$[Ru(bpy)_2(py)_2]^{2+}$ and $[Ru(pmp)_2]^{2+}$ (pmp = 2,6-bis(2-pyridylmethyl)pyridine) compounds was investigated, and the geometrical features of the complexes for the ^{3}MLCT $\rightarrow {}^3$MC transition were assessed. With this knowledge, we thereafter investigated the photochemistry of the newly published $[Ru(bqp)_2]^{2+}$ complex.[22] Three of the previous complexes contain tridentate ligands, and one is closely related (*cis*-$[Ru(bpy)_2(py)_2]^{2+}$) to such a complex, and a mapping of common features of the photoprocesses can therefore be made for this kind of complex. We explain in this paper that high-level quantum-chemical methods and large basis sets are important for capturing the essential features of the first excited triplet state. This is the first high-level study of the most important excited state of ruthenium polypyridyl complexes. This study also provides a good basis for understanding if there is, in reality, any coupling between ligand coordination and thermodynamics of the ^{3}MLCT $\rightarrow {}^3$MC transition.

Materials and Methods

The models used consisted of full ruthenium plus ligands systems. The total charge was kept at +2, and triplet multiplicity was assumed throughout, except for the ground state, where singlet multiplicity was used. All calculations were conducted using density functional theory (DFT) with the B3LYP functional.[22,23] B3LYP is known to perform well for several metal-centered complexes.[24] Many theoretical studies of Ru-centered complexes exist, with different methodologies chosen, ranging from semiempirical[25–27] to gradient-corrected DFT[28] and hybrid functional methods such as PBE0[29–31] and B3LYP.[31–37] The advantage of using a hybrid density functional is that a Hartree−Fock exchange is necessary for obtaining a reliable description of nonlocal same-spin interactions in the triplet state. B3LYP was chosen here since is the most benchmarked functional today.

The basis set dependencies of energies and geometries were thoroughly studied. It was found that double-ζ plus polarization (DZP) quality or better is necessary for obtaining reliable results. LANL2DZ geometries were found to differ considerably from the geometries presented in this work. In geometry optimizations and frequency calculations, the well-known 6-31G(d,p) basis set was used for first and second row atoms, and the SDD basis set was used for ruthenium. To obtain better energies and for the Mulliken spin density analysis, the 6-311G(2df,p) basis set was used for first and second row atoms in subsequent single point calculations. Since the state investigated is not of Rydberg character, nor a typical radical, diffuse functions were not used. The stationary points were confirmed to be either minima or saddle points by performing frequency calculations. Mulliken spin density analysis was used for establishing the nature of the electronic state, a ^{3}MLCT state was associated with a unity net spin on ruthenium, while a net spin of 2 on ruthenium classified the state as ^{3}MC. The results are collected in Table 1.

In some cases, a barrier between two ^{3}MC states could be found, and transition state optimizations were conducted. A major geometrical component of the reaction coordinates in the all transitions investigated is an elongation of the Ru−N bonds. Since these bonds are weak, the curvature of the PES at the corresponding transition states is small, and anharmonic corrections are needed for reliable frequency calculations. In this study, however, reaction barriers are not the major concern, but rather finding reaction coordinates for the different transitions was the goal, the transition from one electronic state to another being reflected in the Ru−N distances. All calculations were performed with the Gaussian 03 suite of programs,[38] and the geometries can be found in the Supporting Information.

Results and Discussion

Classification of Electronic States and Availability of Transitions. The incentive of the present work was to investigate the thermodynamics of four related ruthenium polypyridyl complexes (Figure 2) with significantly different triplet state lifetimes. As a reference compound, the properties of the $[Ru(tpy)_2]^{2+}$ complex were calculated, and the thermodynamics of this compound was compared to the thermodynamics of three other compounds: one molecule obtained when removing two bonds from tpy, *cis*-$[Ru(bpy)_2(py)_2]^{2+}$; a molecule with nearly perfect octahedral coordination of the central ion, $[Ru(pmp)_2]^{2+}$; and a more rigid complex with good Ru coordination, $[Ru(bqp)_2]^{2+}$. In doing so, the nuclear geometries and electronic structures involved in the ^{3}MLCT $\rightarrow {}^3$MC transitions were identified as a means to validate and understand the results of relative energetics of the ^{3}MLCT and ^{3}MC state and also to couple the geometrical alterations to the changes in electronic structure.

As an illustration as to what ligand-field theory provides in the explanation of the stability of the complexes, the frontier

TABLE 1: T_1 Relevant Calculated Parameters[a]

	$[Ru(tpy)_2]^{2+}$	*cis*-$[Ru(bpy)_2(py)_2]^{2+}$	$[Ru(pmp)_2]^{2+}$	$[Ru(bqp)_2]^{2+}$
T_1	^{3}MLCT; ^{3}MC-d_{z^2}	^{3}MLCT; $^3MC_1$; $^3MC_2$; TS	^{3}MLCT; $^3MC_1$; $^3MC_2$; TS_1; TS_2	^{3}MLCT; $^3MC_1$; $^3MC_2$; TS
spin (Ru)	0.93; 1.78	0.98; 1.91; 1.90; 1.85	1.05; 1.86; 1.86; 1.84; 1.84	0.68; 1.78; 1.70; 1.74
charge (Ru)	1.59; 1.17	1.61; 1.14; 1.15; 1.21	1.00; 0.70; 0.71; 0.71; 0.71	0.97; 0.77; 0.80; 0.79
ΔG_g (kcal/mol)	---; −4.0	---; −13.4; −12.1; −6.3	---; −29.8; −23.9; −21.0; −24.1	---; −2.2; −1.6; +0.5
N_{Imag} (cm^{-1})	---; ---	---; ---; ---; −109.7	*b*; ---; ---; −86.2; −73.7	---; ---; ---; ---; −89.4
		Bond lengths (Å)		
r_{A+}	2.117; 2.382	2.112; 2.103; 2.105; 2.114	2.142; 2.185; 2.187; 2.355; 2.398	2.077; 2.166; 2.108; 2.093
r_{A-}	2.086; 2.382	2.112; 2.160; 2.168; 2.114	2.142; 2.185; 2.187; 2.355; 2.398	2.097; 2.086; 2.088; 2.093
r_{B+}	2.105; 2.150	2.192; 2.157; 2.160; 2.436	2.142; 2.557; 2.187; 2.355; 2.311	2.134; 2.165; 2.199; 2.286
r_{B-}	2.116; 2.160	2.066; 2.107; 2.104; 2.250	2.142; 2.557; 2.187; 2.355; 2.311	2.111; 2.140; 2.243; 2.286
r_{C+}	1.998; 2.010	2.066; 2.379; 2.390; 2.251	2.126; 2.192; 2.449; 2.145; 2.141	2.170; 2.505; 2.338; 2.288
r_{C-}	2.046; 2.185	2.192; 3.095; 2.966; 2.445	2.126; 2.135; 2.449; 2.145; 2.152	2.031; 2.433; 2.273; 2.288
		Angles (deg)		
$\upsilon(r_{A+}, r_{C+})$	102.1; 108.7	93.8; 106.5; 105.4; 97.7	91.5; 92.3; 95.1; 93.1; 93.3	88.3; 81.4; 85.3; 86.5
$\upsilon(r_{C+}, r_{A-})$	103.7; 108.7	78.8; 72.6; 72.3; 75.9	91.5; 92.3; 95.1; 93.1; 93.3	91.0; 97.9; 94.3; 93.5
$\upsilon(r_{A-}, r_{C-})$	77.6; 71.7	98.2; 91.4; 91.6; 97.6	88.5; 87.7; 84.9; 86.9; 86.7	88.4; 99.7; 94.5; 93.5
$\upsilon(r_{C-}, r_{A+})$	77.0; 71.7	89.1; 88.8; 89.9; 89.1	88.5; 87.7; 84.9; 86.9; 86.7	88.4; 81.0; 85.9; 86.5
$\upsilon(r_{A+}, r_{B+})$	89.3; 101.7	98.1; 97.4; 97.5; 97.9	82.9; 82.9; 85.6; 82.4; 82.4	91.6; 92.5; 92.8; 93.5
$\upsilon(r_{B+}, r_{A-})$	88.7; 101.6	89.2; 86.7; 87.0; 89.1	97.2; 97.4; 95.3; 98.0; 97.9	89.1; 88.3; 88.0; 86.5
$\upsilon(r_{A-}, r_{B-})$	96.1; 86.0	93.7; 98.2; 97.9; 97.4	82.9; 82.9; 85.6; 82.4; 82.4	88.9; 88.7; 87.0; 86.5
$\upsilon(r_{B-}, r_{A+})$	95.6; 86.0	78.9; 77.7; 77.7; 75.9	97.2; 97.4; 95.3; 98.0; 97.9	90.3; 90.4; 92.2; 93.5

[a] Directions of bonds, along or opposite to the axes indicated in Figure 2, are denoted with + or −, respectively. [b] ^{3}MLCT: −725.5; −345.9; −63.1; −17.8 cm^{-1}.

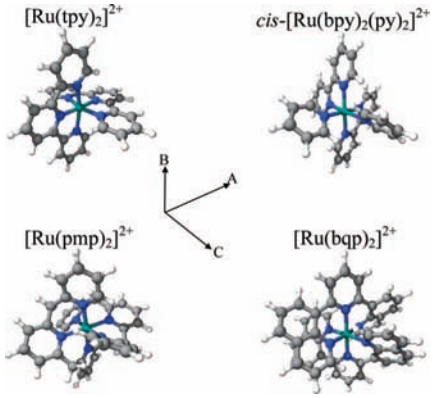

Figure 2. Calculated geometries of the ^{3}MLCT states of the four complexes investigated.

orbital structure of the two extremes ($[Ru(tpy)_2]^{2+}$, $\tau = 0.25$ ns and $[Ru(bqp)_2]^{2+}$, $\tau = 3$ μs) is displayed in Figure 3. The three highest occupied orbitals have contributions of d_{xy}, d_{yz}, and d_{xz} in both complexes. The first Ru−N antibonding orbitals are located more than 5 eV above the HOMO level in $[Ru(tpy)_2]^{2+}$ (with Ru $d_{x^2-y^2}$ and Ru d_{z^2} contributions), while an antibonding orbital with Ru $d_{x^2-y^2}$ character appears already below 3.5 eV in $[Ru(bqp)_2]^{2+}$. The ligand-field splitting is therefore arguably smaller in $[Ru(bqp)_2]^{2+}$ than in $[Ru(tpy)_2]^{2+}$, and a larger ligand-field splitting does not lead to longer lifetimes.

What indeed can be seen from Figure 3 is that the LUMO of $[Ru(bqp)_2]^{2+}$ has almost no contribution of Ru d orbitals, while Ru d/π* mixing is seen in the LUMO of $[Ru(tpy)_2]^{2+}$. This means that the ^{3}MLCT and ^{3}MC states are more different for $[Ru(bqp)_2]^{2+}$ than for $[Ru(tpy)_2]^{2+}$. This mixing of d and π* orbitals might facilitate the transfer of the π* electron to the Ru and thereby the ^{3}MLCT → ^{3}MC transition. On the other hand, the classification of the orbitals is not unambiguous, as both d and π contributions are present in all molecular orbitals, and explicit calculation of the total energy of the states is motivated.

The ^{3}MC state is analyzed with respect to which d* orbitals are contributing to the Ru−N(σ*) orbital. The virtual orbital of

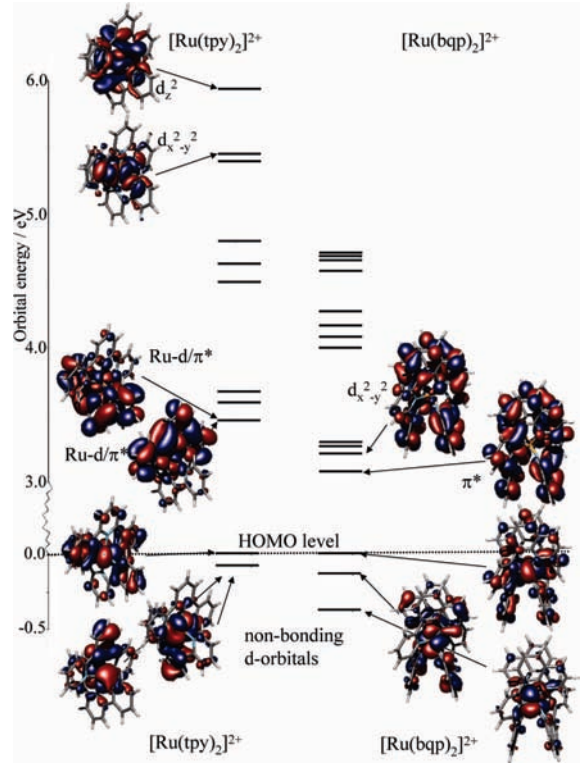

Figure 3. Relevant orbitals of the $[Ru(tpy)_2]^{2+}$ and $[Ru(bqp)_2]^{2+}$ complexes.

(mainly) d character in the ^{3}MC states is antibonding with respect to the Ru−N bonds. Either two opposite or four coplanar Ru−N bonds are elongated upon the ^{3}MLCT → ^{3}MC transition; the d part of the antibonding orbital is either d_{z^2} or $d_{x^2-y^2}$. Rearrangements between different ^{3}MLCT states were not observed in this study. These phenomena have been studied for $[Ru(bpy)_2]^{2+}$,[39,40] where it was investigated as to if the π* electron is localized on one or several ligands. It has, in that complex, been concluded that these rearrangements occur on subpicosecond timescales[40] and, in line with this, that only one

TABLE 2: S_0 Structural Parameters[a]

S_0	$[Ru(tpy)_2]^{2+}$ calcd; exptl[37]	*cis*-$[Ru(bpy)_2(py)_2]^{2+}$ calcd; exptl;[49] exptl-I;[50] exptl-II[50]	$[Ru(pmp)_2]^{2+}$ calcd	$[Ru(bqp)_2]^{2+}$ calcd; calcd;[18] exptl[18]
		Bond lengths (Å)		
r_{A+}	2.115; 2.07	2.121; 1.99(3); 2.079(2); 2.065(7)	2.151	2.085; 2.081; 2.025(17)
r_{A-}	2.115; 2.07	2.121; 2.04(3); 2.085(3); 2.071(6)	2.151	2.085; 2.081; 2.025(17)
r_{B+}	2.115; 2.05	2.172; 2.13(2); 2.126(2); 2.118(7)	2.151	2.120; 2.114; 2.077(16)
r_{B-}	2.116; 2.05	2.098; 2.01(2); 2.075(2); 2.053(7)	2.151	2.120; 2.114; 2.077(16)
r_{C+}	2.012; 1.99	2.099; 2.13(2); 2.059(3); 2.061(6)	2.144	2.120; 2.114; 2.048(17)
r_{C-}	2.013; 1.99	2.171; 2.06(3); 2.112(3); 2.116(7)	2.144	2.120; 2.114; 2.048(17)
		Angles (deg)		
$v(r_{A+}, r_{C+})$	101.6; ---	93.8; 94(1); 95.88(10); 94.8(3)	91.7	89.5; 89.8; 88.9(7)
$v(r_{C+}, r_{A-})$	101.5; ---	77.9; 85(1); 79.05(11); 78.2(3)	91.7	90.5; ---; ---
$v(r_{A-}, r_{C-})$	78.4; 78.6	96.8; 91(1); 99.13(10); 100.5(3)	88.3	90.5; 89.8; 92.1(7)
$v(r_{C-}, r_{A+})$	78.4; 78.6	91.4; 90(1); 86.17(10); 86.3(3)	88.3	89.5; ---; ---
$v(r_{A+}, r_{B+})$	92.4; 91.2	96.8; 99(1); 99.90(9); 99.1(3)	83.6	90.5; ---; ---
$v(r_{B+}, r_{A-})$	92.3; ---	91.5; 86(1); 86.99(9); 86.3(3)	96.5	89.5; ---; ---
$v(r_{A-}, r_{B-})$	92.3; ---	93.7; 98(1); 94.13(9); 95.8(3)	83.6	89.5; ---; ---
$v(r_{B-}, r_{A+})$	92.4; 91.2	78.0; 77(1); 78.78(9); 79.0(3)	96.5	90.5; ---; ---
$v(r_{B+}, r_{A-}) + v(r_{A-}, r_{B-})$	184.6; ---	185.2; 184; 181.12; 182.1	180.1	179.0; 179.6; 177.6(7)

[a] Directions of bonds, along or opposite to the axes indicated in Figure 2, are denoted with + or −, respectively. $[Ru(tpy)_2][Cl_4]\cdot 0.55H_2O$ (ref 37); *cis*-$[Ru(bipy)_2(py)_2][BF_4]_2\cdot 0.5[Hpy][BF_4]$ (ref 49); Δ-[Ru(bpy)$_2$(py)$_2$][(+)-*O*,*O*′-di-benzoyl-D-tartrate]·$12H_2O$ (I) and Λ-[Ru(bpy)$_2$(py)$_2$][(−)-*O*,*O*′-dibenzoyl-L-tartrate]·$12H_2O$ (II) (ref 50); and $[Ru(bqp)_2](PF_6)_2$ (ref 18).

^{3}MLCT structure per complex was observed here, as also has been thoroughly discussed in the literature (see, e.g., ref 41).

Reference $[Ru(tpy)_2]^{2+}$ Complex. It has been claimed that the deviations from octahedral coordination around Ru are responsible for the low photostability of the $[Ru(tpy)_2]^{2+}$ complex.[17,18] This is based upon crystal structures presented both for $[Ru(tpy)_2]^{2+}$,[42] Table 2, and $[Ru(tpy)_2]^0$,[43] the latter presumably geometrically comparable to the ^{3}MLCT structure found here since the lowest π^* orbitals of tpy accept the extra electrons upon reduction. An assessment of the quality of the calculated geometries was performed here by comparing the bond distances of S_0 to those of the crystal structure of $[Ru(tpy)_2]^{2+}$.

Previously, DFT studies employing the LANL2DZ basis set were presented for the ground state,[37,44] while the lowest triplet state was optimized at the ZINDO/S level.[45] For an initial screening of the triplet multiplicity PES, the LANL2DZ basis set was used also in this study, which resulted in several stationary points in the first triplet state, which were not found when larger basis sets were employed. Therefore, no conclusions were drawn from calculations employing the LANL2DZ basis set. All calculations, even on S_0, were therefore performed using DZP basis sets. In the notation used next, the axes *A*, *B*, and *C* are defined in Figure 2 with a + sign in the direction of the axes. The relevant geometrical parameters as well as energetics are given in Table 1 for the triplets, while in Table 2, we present the geometrical parameters for the singlets.

Ru−N bond distances are slightly overestimated. Comparing the S_0 calculated structure with the experimental crystal structure (Table 2), four coplanar bonds are 2.116 Å (r_{B-}) and 2.115 Å (r_{A+}, r_{A-}, and r_{B+}) in the calculations, while experimentally are 2.07 Å (r_{A+}, r_{A-}) and 2.05 Å (r_{B+}, r_{B-}). The axial bonds (r_{C+}, r_{C-}) are overestimated by only 0.023 and 0.022 Å (i.e., 2.013 and 2.012 Å as compared to the experimental 1.99 Å). Overall, the bond length deviations are about 1%, and the errors are significantly smaller than the changes in geometry upon excitation and ^{3}MLCT → ^{3}MC deactivation.

Given this benchmark, we turn to the more significant T_1 state, which we investigated using the standard, time-independent, DFT method. Time-dependent (TD)-DFT, which is normally chosen for excited states, has inherent problems in describing CT states since electron self-interaction was not properly corrected for in a Kohn−Sham[46] scheme employing local exchange interactions.[47] Great care therefore needs to be taken when, for example, calculating excitation spectra since comparing charge transfer (CT) states (such as ^{3}MLCT) with locally excited (LE) states (such as ^{3}MC) is dubious. Since ^{3}MLCT is clearly CT type, TD-DFT is avoided here. There are, however, examples of the successful application of TD-DFT in describing MLCT states in Ru(II) complexes in the literature.[48] On the other hand, ab initio schemes, such as configuration interaction singles (CIS), greatly overestimate excitation energies, and more correlated methods are still too expensive today. Therefore, DFT in a time-independent formalism is today the most feasible method for an extensive PES investigation of this kind of system, given that it is the lowest triplet state that is studied.

Upon optimization of the excited-state geometry, the Ru−N bond distances do not change much. In Figure 2, the optimized ^{3}MLCT structure is displayed, with relevant geometrical parameters describing the coordination around the Ru atom in Table 1. The coordination of the ruthenium atom is almost unaltered in ^{3}MLCT as compared to the S_0 structures. The largest bond−distance changes are in r_{A-} (−0.029 Å) and r_{C-} (+0.033 Å). No angle is changed more than 4°. These small alterations imply that the Ru−N bond order does not change upon excitation and that both the singly occupied d orbital and the π^* are nonbonding with respect to all Ru−N distances.

The ^{3}MLCT state of this molecule is very short-lived with $\tau = 0.25$ ns.[21] With this short lifetime, the level of theory does not allow explicit transition state optimization of a presumed ^{3}MLCT → ^{3}MC barrier. The geometrical changes following the ^{3}MLCT → ^{3}MC transition imply that the electronic rearrangements that accompany these nuclear movements are $d\pi^* \rightarrow dd_{x^2-y^2}$ in character. This conclusion is drawn since the major changes are in the four coplanar Ru−N bonds, r_B and r_A. One of the r_C bonds is, however, also significantly changed (from 1.998 and 2.046 Å to 2.010 and 2.185 Å, respectively). The major alteration of r_{C-} might suggest that d_{z^2} mixes with $d_{x^2-y^2}$.

After analyzing both ^{3}MLCT and ^{3}MC states, the crystal structure of $[Ru(tpy)_2]^0$ (ref 37) can be identified as resembling the ^{3}MLCT state. Two different isomers are presented in ref 37, and they are similar with respect to Ru−N distances, with

r_C very similar (1.98 and 2.00 Å) to the ^{3}MLCT structures obtained here (1.998 and 2.046 Å). The calculated r_A distances are slightly longer, 2.117 and 2.086 Å, as compared to 2.05 and 2.09 Å, respectively, and the same is true for r_B, experimentally, 2.06 and 2.08 Å, and calculated, 2.105 and 2.116 Å, respectively. The larger discrepancies in the r_B distances are most likely due to mixing between the antibonding Ru(d_{z^2})−N(n*) orbital of σ* character with tpy π* in the excited state but not in the reduced species, where only π* is occupied.

The ^{3}MC state is slightly lower in energy than the ^{3}MLCT state ($\Delta G_g = -4.0$ kcal/mol), which, as seen in experiments, implies that it is thermodynamically accessible from ^{3}MLCT at room temperature. The Mulliken analysis is in good agreement with the qualitative picture of the spin and charge of ruthenium. In the ^{3}MLCT state, the spin density on Ru is 0.93, which is essentially unity, and the charge is +1.59, which is reasonably close to +2. In the ^{3}MC state, one electron is transferred to ruthenium, and the spin density has changed by approximately one unit, to 1.78, and the charge to unity (1.17). The estimates of the spin are, as expected, better than that of the charges since the spin is calculated as the difference between α and β spin densities, $\rho_\alpha - \rho_\beta$, and a cancelation of errors occurs.

Improvement of Ligand Coordination – *cis*-[Ru(bpy)$_2$-(py)$_2$]$^{2+}$ Complex. An early experimental investigation of the *cis*-[Ru(bpy)$_2$(py)$_2$]$^{2+}$ complex was undertaken by Durham and co-workers,[49] and perhaps the most important result there, for this work, is that the lifetime of the lowest triplet state is 500 ns. At first glance, this might be surprising since the only structural difference from [Ru(tpy)$_2$]$^{2+}$ is that the ligands contain one bond less, and this increases the lifetime by a factor of 2000. This makes this complex a good model to test the influence of coordination of the central metal ion, with a minimum of alteration of the ligand.

Regarding the S_0 structure of *cis*-[Ru(bpy)$_2$(py)$_2$]$^{2+}$, crystal structures for *cis*-[Ru(bpy)$_2$(py)$_2$][BF$_4$]$_2$·0.5[Hpy][BF$_4$] were presented by Zora et al.[50] and for Δ-[Ru(bpy)$_2$(py)$_2$][(+)-*O*,*O*′-dibenzoyl-D-tartrate]·12H$_2$O and Λ-[Ru(bpy)$_2$(py)$_2$][(−)-*O*,*O*′-dibenzoyl-L-tartrate]·12H$_2$O by Kolp et al.[51] Comparing these three crystal structures with the calculated one, we see that the bond lengths are, as for [Ru(tpy)$_2$]$^{2+}$, slightly overestimated. The comparison is not fully pertinent since vacuum calculations cannot capture the effects of the surrounding crystal, but still, this is the best comparison we can make without detailed knowledge about the surroundings of the complex in the crystal. As compared to Zora et al.'s structure, the root-mean-squared deviation was 0.09 Å for the six Ru−N distances, while a closer resemblance was found as compared to Kolp et al.'s structures, with a root-mean-squared deviation of 0.04 and 0.05 Å. That is, with a bond distance of about 2 Å, the deviation is only 2−3%.

In Figure 2, the calculated ^{3}MLCT structure is displayed, and relevant geometrical parameters are given in Table 1. As for the lowest triplet excitation in [Ru(tpy)$_2$]$^{2+}$, the Ru coordination is not extensively affected. The largest change of a Ru−N distance amounts to −0.033 Å. The ^{3}MLCT state of *cis*-[Ru(bpy)$_2$(py)$_2$]$^{2+}$ displays slightly smaller deviations from octahedral coordination than [Ru(tpy)$_2$]$^{2+}$ does: the root-mean-squared deviation from 90° is 9.5° for [Ru(tpy)$_2$]$^{2+}$ and 7.2° for *cis*-[Ru(bpy)$_2$(py)$_2$]$^{2+}$. The energetics implies that the ^{3}MC state, as for [Ru(tpy)$_2$]$^{2+}$, is more stable than the ^{3}MLCT state. The lowest ^{3}MC state is 13.4 kcal/mol lower in energy than the ^{3}MLCT state in *cis*-[Ru(bpy)$_2$(py)$_2$]$^{2+}$. Taken together, this complex has a longer lifetime than [Ru(tpy)$_2$]$^{2+}$, but the coordination is more or less the same for the two complexes.

Unfortunately, explicit optimization of a ^{3}MLCT → ^{3}MC transition state with sufficient accuracy is not within reach of the computationally feasible methods, but an assumption here can be that this transition should be kinetically, rather than thermodynamically, controlled. The kinetics would in this case be modeled in terms of adiabatic transition state energy (Arrhenius-type reaction) or in terms of nonadiabatic coupling of the electronic states, which can be significant in the context of excited states.

In the analysis of the photostability, we note that one Ru−N bond is not altered alone, and neither are the two in cis positions, but that the geometrical alterations are in two opposite bonds, as the geometry of d_{z^2}, or in four coplanar ones, as in $d_{x^2-y^2}$. Accordingly, we can therefore by means of a simple orbital model explain as to why two of the ligands are of a free monodentate type, which does not largely affect the photostability, when compared to the structurally related [Ru(bpy)$_3$]$^{2+}$ (τ = 890−1150 ns).[15,17]

Tridentate Ligand with Good Octahedral Coordination – [Ru(pmp)$_2$]$^{2+}$ Complex. To further improve the ligand coordination, we ran calculations using a methyl-bridged tridentate ligand, pmp (Figure 2, parameters in Tables 1 and 2). This is a compound that, to the best of our knowledge, has not been experimentally investigated, but it is a way of assessing the effect of nearly perfect ligand coordination on the ^{3}MLCT/^{3}MC thermodynamics.

As to the possible S_0 structure, we found a structure that is very symmetric in which equatorial nitrogen atoms lie at 2.151 Å (r_{A+}, r_{A-}, r_{B+}, r_{B-}) from the metal center, while the axial nitrogen atoms (r_{C+}, r_{C-}) lie at 2.144 Å. Furthermore, this structure is ca. 40 kcal/mol below the most stable T_1 ^{3}MC product found.

In the search for T_1 excited-state structures, and in the search for a ^{3}MLCT structure, we found a very symmetrical species with four short equatorial distances (2.142 Å) and two short axial distances (2.126 Å). This structure, though, does not correspond to a minimum and presents four imaginary frequencies (−725.5; −345.9; −63.1; −17.8 cm^{-1}). While the last one is negligible, the others are not, and every attempt to reoptimize this third order saddle point led to a ^{3}MC structure. This was the only ^{3}MLCT structure that could be found, and it is included as a reference for the ^{3}MC structures.

Four ^{3}MC structures were found, identified either as minima or as first order saddle points. Regarding the ^{3}MC minima, two structures were found, one more symmetric, ^{3}MC$_2$ (with four identical equatorial distances, (r_{A+}, r_{A-}, r_{B+}, r_{B-}) = 2.187 Å, and two identical axial distances, (r_{C+}, r_{C-}) = 2.449 Å), and less stable than the other, ^{3}MC$_1$ (by 5.9 kcal/mol). Both are of the ^{3}MC type and are characterized as minima. These two structures seem to have contributions of both $d_{x^2-y^2}$ and d_{z^2} orbitals in the antibonding Ru−N (σ*) orbitals in both structures, which explains as to why they have this type of coordination, with all six bonds elongated, as compared to the parent S_0, and as to why no structures showing essentially only $d_{x^2-y^2}$ or d_{z^2} occupation were found.

Finally, we stress that the absence of a ^{3}MLCT stationary point in our calculations does not necessarily mean that it does not exist. What can be said, however, is that the large flexibility of the ligands, due to the methane bridges, might imply that the geometrical distortions for the ^{3}MLCT → ^{3}MC transition are easily obtained. Also, these methane bridges imply a loss

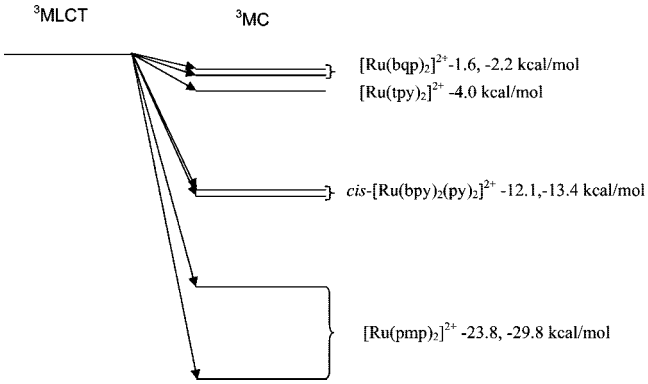

Figure 4. Energetics of the ^{3}MLCT and ^{3}MC states. The ^{3}MLCT state of the respective complex is chosen as the zero level.

of conjugation and consequently should imply a destabilization of the ^{3}MLCT state.

New Alternative – $[Ru(bqp)_2]^{2+}$ Complex. Good coordination and more rigidity are introduced with the bqp ligands. This compound has been synthesized and was recently published.[18] For this family, we found a structure for the S_0 ground state (Table 2), several structures for the T_1 excited state, a ^{3}MLCT minimum (Figure 2 and Table 1), and two ^{3}MC minima. Further, several ^{3}MC-type first order saddle points were found.

Regarding the S_0 structure, this can be compared with the experimental structure and with the one obtained at the B3LYP/LANL2DZ level.[18] As for the calculated LANL2DZ structure, the distances are slightly overestimated when compared with the experimental values, while our angles compare better with the crystal structure than the ones from the calculated structure in ref 18 do. For instance, we mention here first our results and then the experimental and last LANL2DZ, respectively (also given in Table 2); $v(r_{A+}, r_{C+}) = 89.5$, 88.9(7) exptl,[18] 89.8 calcd;[18] $v(r_{A-}, r_{C-}) = 90.5$, 92.1(7) exptl,[18] 89.8 calcd;[18] and $v(r_{B+}, r_{A-}) + v(r_{A-}, r_{B-}) = 179.0$, 177.6(7) exptl,[18] 179.6 calcd.[18] The overall calculated structure is more symmetric than the one in the crystal. It lies approximately 40 kcal/mol below the T_1 ^{3}MC minima found (as observed also in the case of the $[Ru(pmp)_2]^{2+}$ family). In the investigation of the T_1 states, we found a surprisingly asymmetric minimum, a ^{3}MLCT structure. The relevance of not relying on the S_0 structure is apparent in this case, as the geometries are distorted upon excitation (equatorial bonds $(r_{B+}, r_{B-}, r_{C+}, r_{C-}) = 2.120$ Å are distorted to 2.134, 2.111, 2.170, and 2.031 Å, respectively, and the axial bonds $(r_{A+}, r_{B+}) = 2.085$ Å are distorted to 2.077 and 2.097 Å, respectively).

Two structures of the ^{3}MC type were identified as minima, and none of them is very symmetric, of which one, $^3MC_2$-$d_{x^2-y^2}$, is less stable (by 0.6 kcal/mol) than the other, $^3MC_1$-d_{z^2} (lies under the ^{3}MLCT minimum energy by −2.2 kcal/mol). Having a good octahedral coordination implies that the d_{z^2} and $d_{x^2-y^2}$ ^{3}MC structures become nearly degenerate.

Pictorial PES. Octahedral coordination of the Ru center, which is well-known to lead to destabilization of the unoccupied Ru d orbitals, does not lead to destabilization of the ^{3}MC state. This study therefore shows that it is necessary to go beyond the simple ligand-field splitting model when investigating the stability of ^{3}MLCT states. Factors other than the thermodynamics of the stationary points are therefore important for photostability. Complexes with significantly different lifetimes display more or less the same thermodynamic pattern. The summarizing pictorial PES in Figure 4 shows that all ^{3}MC states are lower in energy than the corresponding ^{3}MLCT state and that the ^{3}MC state of the most stable molecule, $[Ru(bqp)_2]^{2+}$, indeed is most stable (−1.6 kcal/mol) but insignificantly more stable than that of the least stable molecule, $[Ru(tpy)_2]^{2+}$ (−4.0 kcal/mol).

Conclusion

We investigated the first excited triplet state of four ruthenium polypyridyl complexes, $[Ru(tpy)_2]^{2+}$, *cis*-$[Ru(bpy)_2(py)_2]^{2+}$, $[Ru(pmp)_2]^{2+}$, and $[Ru(bqp)_2]^{2+}$ by means of DFT. We assessed the short-lived, and thereby experimentally inaccessible, excited-state structures important for the photoactivity of these complexes. Four important conclusions were made: (i) The geometrical alterations during ^{3}MLCT → ^{3}MC and ^{3}MC → ^{3}MC transitions can be explained by which Ru d orbital (e_g) is being occupied, which is the one that contains d_{z^2} or $d_{x^2-y^2}$ contributions. Two axial bonds are changed if it is d_{z^2} and four coplanar if it is $d_{x^2-y^2}$. (ii) This study shows that it is necessary to go beyond the simple ligand-field splitting model when investigating the stability of the ^{3}MLCT states, as referred to before. It has been shown that the thermodynamics of the stationary points is not the only important factor for photostability. (iii) When comparing the pmp family with the bqp family, both showing very good coordination, we can assume that single bonds in the ligands should be avoided since they lead to a larger flexibility of the structure, possibly inducing easier access to the deactivation pathway. (iv) On the computational side, at least a double-ζ polarization basis is needed for an accurate description of the triplet state. Using the spin at the Ru center as a means of identifying the electronic state, we see that a coupling between experiments and calculations at this level of theory can be made. Experimental (S_0) structures are well-reproduced (bond lengths within 2% around Ru) using the B3LYP/6-31G(d,p) (C,N,H) SDD (Ru) approach.

We have in this paper presented a reliable level of theory for these calculations and, in addition, shown that it is worthwhile to go beyond the ligand-field splitting orbital model to obtain quantitative measures of relative stability and thus determine geometrical features defining ^{3}MLCT and different ^{3}MC states. This, in turn, provides further insight needed for the understanding of the photostability of these complexes.

Supporting Information Available: Geometries of stationary points (in Å). This information is available free of charge via the Internet at http://pubs.acs.org.

Acknowledgment. This work was supported by the Swedish Research Council (VR) and the Göran Gustafsson Foundation. The Swedish supercomputer center NSC is gratefully acknowledged for the generous supply of computer resources. S.S.M. C.G. also thanks the Portuguese Science and Technology Foundation (FCT) for a postdoctoral grant (SFRH/BPD/29659/2006).

References and Notes

(1) Meyer, T. J. *Acc. Chem. Res.* **1989**, *22*, 163–170.
(2) Hammarström, L. *Curr. Opin. Chem. Biol.* **2003**, *7*, 666–673.
(3) O'Regan, B.; Grätzel, M. *Nature (London, U.K.)* **1991**, *353*, 737–740.
(4) Hagfeldt, A.; Grätzel, M. *Acc. Chem. Res.* **2000**, *33*, 269–277.
(5) Nazeeruddin, M. K.; Pechy, P.; Renouard, T.; Zakeeruddin, S. M.; Humphry-Baker, R.; Comte, P.; Liska, P.; Cevey, L.; Costa, E.; Shklover, V.; Spiccia, L.; Deacon, G. B.; Bignozzi, C. A.; Grätzel, M. *J. Am. Chem. Soc.* **2001**, *123*, 1613–1624.
(6) Alstrum-Acevedo, J. H.; Brennaman, M. K.; Meyer, T. J. *Inorg. Chem.* **2005**, *44*, 6802–6827.
(7) Falkenström, M.; Johansson, O.; Hammarström, L. *Inorg. Chim. Acta* **2007**, *360*, 741–750.

(8) Johansson, A.; Abrahamsson, M.; Magnuson, A.; Huang, P.; Mårtensson, J.; Styring, S.; Hammarström, L.; Sun, L.; Åkermark, B. *Inorg. Chem.* **2003**, *42*, 7502–7511.

(9) Berg, K. E.; Tran, A.; Raymond, M. K.; Abrahamsson, M.; Wolny, J.; Redon, S.; Andersson, M.; Sun, L.; Styring, S.; Hammarström, L.; Toftlund, H.; Åkermark, B. *Eur. J. Inorg. Chem.* **2001**, *2001*, 1019–1029.

(10) Borgström, M.; Johansson, O.; Lomoth, R.; Berglund Baudin, H.; Wallin, S.; Sun, L.; Åkermark, B.; Hammarström, L. *Inorg. Chem.* **2003**, *42*, 5173–5184.

(11) Abrahamsson, M. L. A.; Berglund Baudin, H.; Tran, A.; Philouze, C.; Berg, K. E.; Raymond-Johansson, M. K.; Sun, L.; Åkermark, B.; Styring, S.; Hammarström, L. *Inorg. Chem.* **2002**, *41*, 1534–1544.

(12) Wolpher, H.; Borgström, M.; Hammarström, L.; Bergquist, J.; Sundström, V.; Styring, S.; Sun, L.; Åkermark, B. *Inorg. Chem. Commun.* **2003**, *6*, 989–991.

(13) Borgström, M.; Shaikh, N.; Johansson, O.; Anderlund, M. F.; Styring, S.; Åkermark, B.; Magnuson, A.; Hammarström, L. *J. Am. Chem. Soc.* **2005**, *127*, 17504–17515.

(14) Polo, A. S.; Itokazu, M. K.; Iha, N. Y. M. *Coord. Chem. Rev.* **2004**, *248*, 1343–1361.

(15) Juris, A.; Balzani, V.; Barigelletti, F.; Campagna, S.; Belser, P.; Vonzelewsky, A. *Coord. Chem. Rev.* **1988**, *84*, 85–277.

(16) Fan, J.; Tysoe, S.; Strekas, T. C.; Gafney, H. D.; Serpone, N.; Lawless, D. *J. Am. Chem. Soc.* **1994**, *116*, 5343–5351.

(17) Abrahamsson, M.; Wolpher, H.; Johansson, O.; Larsson, J.; Kritikos, M.; Eriksson, L.; Norrby, P. O.; Bergquist, J.; Sun, L. C.; Åkermark, B.; Hammarström, L. *Inorg. Chem.* **2005**, *44*, 3215–3225.

(18) Abrahamsson, M.; Jäger, M.; Österman, T.; Eriksson, L.; Persson, P.; Becker, H. C.; Johansson, O.; Hammarström, L. *J. Am. Chem. Soc.* **2006**, *128*, 12616–12617.

(19) Berglund Baudin, H.; Davidsson, J.; Serroni, S.; Juris, A.; Balzani, V.; Campagna, S.; Hammarström, L. *J. Phys. Chem. A* **2002**, *106*, 4312–4318.

(20) Pomeranc, D.; Heitz, V.; Chambron, J. C.; Sauvage, J. P. *J. Am. Chem. Soc.* **2001**, *123*, 12215–12221.

(21) Sauvage, J. P.; Collin, J. P.; Chambron, J. C.; Guillerez, S.; Coudret, C.; Balzani, V.; Barigelletti, F.; Decola, L.; Flamigni, L. *Chem. Rev.* **1994**, *94*, 993–1019.

(22) Becke, A. D. *J. Chem. Phys.* **1993**, *98*, 5648–5652.

(23) Lee, C. T.; Yang, W. T.; Parr, R. G. *Phys. Rev. B: Condens. Matter Mater. Phys.* **1988**, *37*, 785–789.

(24) Siegbahn, P. E. M. *J. Biol. Inorg. Chem.* **2006**, *11*, 695–701.

(25) Ershov, A. Y.; Shashko, A. D.; Sizova, O. V.; Ivanova, N. V.; Burov, S. V.; Kuteikina-Teplyakova, A. V. *Russ. J. Gen. Chem.* **2003**, *73*, 135–140.

(26) Pourtois, G.; Beljonne, D.; Moucheron, C.; Schumm, S.; Kirsch-De Mesmaeker, A.; Lazzaroni, R.; Bredas, J. L. *J. Am. Chem. Soc.* **2004**, *126*, 683–692.

(27) Broo, A.; Lincoln, P. *Inorg. Chem.* **1997**, *36*, 2544–2553.

(28) Fantacci, S.; De Angelis, F.; Selloni, A. *J. Am. Chem. Soc.* **2003**, *125*, 4381–4387.

(29) Guillemoles, J. F.; Barone, V.; Joubert, L.; Adamo, C. *J. Phys. Chem. A* **2002**, *106*, 11354–11360.

(30) Aiga, F.; Tada, T. *Sol. Energy Mater. Sol. Cells* **2005**, *85*, 437–446.

(31) Monat, J. E.; Rodriguez, J. H.; McCusker, J. K. *J. Phys. Chem. A* **2002**, *106*, 7399–7406.

(32) Stoyanov, S. R.; Villegas, J. M.; Rillema, D. P. *Inorg. Chem.* **2002**, *41*, 2941–2945.

(33) Singh, A.; Chandra, M.; Sahay, A. N.; Pandey, D. S.; Pandey, K. K.; Mobin, S. M.; Puerta, M. C.; Valerga, P. *J. Organomet. Chem.* **2004**, *689*, 1821–1834.

(34) Zheng, K. C.; Wang, J. P.; Peng, W. L.; Liu, X. W.; Yun, F. C. *J. Mol. Struct.* **2002**, *582*, 1–9.

(35) Xie, Z. Z.; Fang, W. H. *J. Mol. Struct.* **2005**, *717*, 179–187.

(36) Gorelsky, S. I.; Lever, A. B. P. *J. Organomet. Chem.* **2001**, *635*, 187–196.

(37) Zhou, X.; Ren, A. M.; Feng, J. K. *J. Organomet. Chem.* **2005**, *690*, 338–347.

(38) Frisch, M. J. ; Trucks, G. W.; Schlegel, H. B.; Scuseria, G. E.; Robb, M. A.; Cheeseman, J. R.; Montgomery, J. A., Jr.; Vreven, T.; Kudin, K. N.; Burant, J. C.; Millam, J. M.; Iyengar, S. S.; Tomasi, J.; Barone, V.; Mennucci, B.; Cossi, M.; Scalmani, G.; Rega, N.; Petersson, G. A.; Nakatsuji, H.; Hada, M.; Ehara, M.; Toyota, K.; Fukuda, R.; Hasegawa, J.; Ishida, M.; Nakajima, T.; Honda, Y.; Kitao, O.; Nakai, H.; Klene, M.; Li, X.; Knox, J. E.; Hratchian, H. P.; Cross, J. B.; Bakken, V.; Adamo, C.; Jaramillo, J.; Gomperts, R.; Stratmann, R. E.; Yazyev, O.; Austin, A. J.; Cammi, R.; Pomelli, C.; Ochterski, J. W.; Ayala, P. Y.; Morokuma, K.; Voth, G. A.; Salvador, P.; Dannenberg, J. J.; Zakrzewski, V. G.; Dapprich, S.; Daniels, A. D.; Strain, M. C.; Farkas, O.; Malick, D. K.; Rabuck, A. D.; Raghavachari, K.; Foresman, J. B.; Ortiz, J. V.; Cui, Q.; Baboul, A. G.; Clifford, S.; Cioslowski, J.; Stefanov, B. B.; Liu, G.; Liashenko, A.; Piskorz, P.; Komaromi, I.; Martin, R. L.; Fox, D. J.; Keith, T.; Al-Laham, M. A.; Peng, C. Y.; Nanayakkara, A.; Challacombe, M.; Gill, P. M. W.; Johnson, B.; Chen, W.; Wong, M. W.; Gonzalez, C.; Pople, J. A. *Gaussian 03, Revision B.05*;Gaussian, Inc.: Wallingford, CT, 2003.

(39) Malone, R. A.; Kelley, D. F. *J. Chem. Phys.* **1991**, *95*, 8970–8976.

(40) (a) Wallin, S.; Davidsson, J.; Modin, J.; Hammarström, L. *J. Phys. Chem. A* **2005**, *109*, 4697–4704. (b) Ibid, J. Phys. Chem. A 2005, *109*, 9378.

(41) Yeh, A. T.; Shank, C. V.; McCusker, J. K. *Science (Washington, DC, U.S.)* **2000**, *289* (5481), 935–938.

(42) Craig, D. C.; Scudder, M. L.; McHale, W. A.; Goodwin, H. A. *Aust. J. Chem.* **1998**, *51*, 1131–1139.

(43) Pyro, S.; Perez-Cordero, E.; Bott, S. G.; Echegoyen, L. *Inorg. Chem.* **1999**, *38*, 3337–3343.

(44) Ciofini, I.; Laine, P. P.; Bedioui, F.; Adamo, C. *J. Am. Chem. Soc.* **2004**, *126*, 10763–10777.

(45) Amini, A.; Harriman, A.; Mayeux, A. *Phys. Chem. Chem. Phys.* **2004**, *6*, 1157–1164.

(46) Kohn, W.; Sham, L. J. *Phys. Rev.* **1965**, *140*, 1133−1138.

(47) Dreuw, A.; Head-Gordon, M. *J. Am. Chem. Soc.* **2004**, *126*, 4007–4016.

(48) Nazeeruddin, M. K.; De Angelis, F.; Fantacci, S.; Selloni, A.; Viscardi, G.; Liska, P.; Ito, S.; Takeru, B.; Grätzel, M. *J. Am. Chem. Soc.* **2005**, *127*, 16835–16847.

(49) Durham, B.; Caspar, J. V.; Nagle, J. K.; Meyer, T. J. *J. Am. Chem. Soc.* **1982**, *104*, 4803–4810.

(50) Hitchcock, P. B.; Seddon, K. R.; Turp, J. E.; Yousif, Z. Y.; Zora, J. A. *J. Chem. Soc., Dalton Trans.* **1988**, 1837–1842.

(51) Kolp, B.; Viebrock, H.; von Zelewsky, A.; Abeln, D. *Inorg. Chem.* **2001**, *40*, 1196–1198.

JP8000702